JPET Fast Forward. Published on January 12, 2004 as DOI:10.1124/jpet.103.060814

JPET #60814

NNC 55-0396: A NEW SELECTIVE INHIBITOR OF T-TYPE CALCIUM CHANNELS

Luping Huang[1], Brian M. Keyser[1], Tina M. Tagmose[2], J. Bondo Hansen[2], James T. Taylor[1], Hean Zhuang[3], Min Zhang[4], David S. Ragsdale [5] and Ming Li[1]

[1]Departments of Pharmacology, Tulane University Health Science Center, New Orleans, LA 70112 (LH, BMK, JTT, ML); [2]Medicinal Chemistry, Novo Nordisk A/S, Måløv, Denmark (TMT, JBH); [3]Department of Anesthesiology and Critical Care Medicine, Johns Hopkins University, Baltimore, Maryland 21217(HZ); [4]Department of Pharmacology, Medical College of Virginia, Richmond, VA 23298 (MZ) and [5]Department of Neurology and Neurosurgery, Montreal Neurological Institute, McGill University, Montreal, Quebec, H3A 2B4 (DSR).

Running Title
Selective T-type Ca^{2+} channel blocker

Correspondence to Ming Li, Ph.D.
Address: Departments of Pharmacology SL-83, 1430 Tulane Avenue, New Orleans, LA 70112, USA.
Phone: (504) 988-8207.
Fax: (504) 588-5283.
E-mail: mli@tulane.edu

Statistics:

Number of	Text pages	20
	Table	0
	Figures	7
	References	21
Words in	Abstract	242
	Introduction	550
	Discussion	366

Non-standard abbreviations:

NNC 55-0395, (1S,2S)-2-(2-(N-[(3-benzoimidazol-2-yl)propyl]-N-methylamino)ethyl)-6-fluoro-1,2,3,4-tetrahydro-1-isopropyl-2-naphtyl valeroate dihydrochloride).

NNC 55-0396, (1S,2S)-2-(2-(N-[(3-benzoimidazol-2-yl)propyl]-N-methylamino)ethyl)-6-fluoro 1,2,3,4-tetrahydro-1-isopropyl-2-naphtyl cyclopropanecarboxylate dihydrochloride.

NNC 55-0397, (1S,2S)-2-(2-(N-[(3-benzoimidazol-2-yl)propyl]-N-methylamino)ethyl)-6-fluoro-1,2,3,4-tetrahydro-1-isopropyl-2-naphtyl isobutyrate dihydrochloride.

Dm-mibefradil, (1S,2S)-2-(2-(N-[(3-benzoimidazol-2-yl)propyl]-N-methylamino)ethyl)-6-fluoro-1,2,3,4-tetrahydro-1-isopropyl-2-naphtyl hydroxy dihydrochloride.

BAPTA, 1,2-bis(2-aminophenoxy)ethane-N, N, N' N'-tetraacetate

JPET Fast Forward. Published on January 12, 2004 as DOI: 10.1124/jpet.103.060814
This article has not been copyedited and formatted. The final version may differ from this version.

Abstract

Mibefradil is a Ca^{2+} channel antagonist, which inhibits both T-type and high-voltage-activated Ca^{2+} channels. We previously showed that block of high-voltage-activated channels by mibefradil occurs through production of an active metabolite by intracellular hydrolysis. In the present study, we modified the structure of mibefradil, to develop a non-hydrolysable analogue, NNC 55-0396, which exerts a selective inhibitory effect on T-type channels. The acute IC_{50} of NNC 55-0396 to block recombinant α_1G T-type channels in HEK293 cells was ~7 μM, whereas 100 μM NNC 55-0396 had no detectable effect on high voltage-activated channels in INS-1 cells. NNC 55-0396 did not affect the voltage-dependent activation of T-type Ca^{2+} currents, but changed the slope of the steady-state inactivation curve. Block of T-type Ca^{2+} current was partially relieved by membrane hyperpolarization and was enhanced at high stimulus frequency. Washing NNC 55-0396 out of the recording chamber did not reverse the T-type Ca^{2+} current activity, suggesting that the compound dissolves in or passes through the plasma membrane to exert its effect; however, intracellular perfusion of the compound did not block T-type Ca^{2+} currents, arguing against a cytoplasmic route of action. After incubating INS-1 cells with NNC 55-0396 for 20 minutes, mass spectrometry did not detect the mibefradil metabolite that causes L-type Ca^{2+} channel inhibition. We conclude that NNC 55-0396, by virtue of its modified structure, does not produce the metabolite that causes inhibition of L-type Ca^{2+} channel channels, thus rendering it more selective to T-type Ca^{2+} channels.

JPET Fast Forward. Published on January 12, 2004 as DOI: 10.1124/jpet.103.060814
This article has not been copyedited and formatted. The final version may differ from this version.

Voltage-gated Ca^{2+} channels are transmembrane proteins involved in the regulation of cellular excitability and intracellular Ca^{2+} signaling. Calcium channels have been divided into various categories, based on functional and pharmacological criteria. High-voltage-activated (HVA) channels, which have been further subdivided into L-, N-, P/Q- and R-types, require strong depolarizations for activation, whereas low-voltage-activated or T-type channels activate over a much more negative voltage range and exhibit unique inactivation and deactivation kinetics (Armstrong and Matteson 1985; Perez-Reyes 1998; Catterall 1998). The main structural component of the voltage-gated calcium channel is the α_1 subunit, which forms the pore and the channel gates. Molecular cloning has identified 10 α_1 subtypes. α_1A-α_1E and α_1S encode HVA channels, whereas α_1G-α_1I encode T-type channels. Pharmacological agents that act selectively on α_1 subtypes have been the key to the study of calcium channel function in many physiological systems; however, a selective antagonist of T-type Ca^{2+} channels is not yet available.

Mibefradil, a tetralol derivative chemically distinct from other Ca^{2+} channel antagonists, has been reported to block T-type Ca^{2+} channel currents in many tissues, including heart (Madle et al, 2001), brain (McDonough et al, 1998), and vascular smooth muscle (Bian et al, 1993; Mishra and Hermsmeyer 1994; Schmitt et al., 1995). Mibefradil was also reported to block HVA Ca^{2+} channels including α_1A, α_1B, α_1C, α_1E (Bezprozvanny and Tsien 1995; Jiménez et al., 2000). We previously demonstrated that mibefradil potently blocked HVA Ca^{2+} channels in a rat insulin secreting cell line (INS-1 cells) via a mechanism involving intracellular hydrolysis of mibefradil to produce an active metabolite (Wu et al., 2000).

The cardiovascular effects of mibefradil are interesting. It decreased heart rate without a

negative inotropic effect (Osterrieder and Holck 1989; Cremers et al., 1997), and its action was not associated with reflex activation of neurohormonal and sympathetic systems (Ernst and Kelly 1998). These properties differ from other clinically important Ca^{2+} antagonists such as nifedipine, diltiazem and verapamil, which in heart selectively inhibit L-type (α_1C) Ca^{2+} channels. However, it is unclear whether the unique effects of mibefradil are caused by the blockade of T-type Ca^{2+} channels, since mibefradil also blocks the L-type Ca^{2+} currents in the cardiomyocytes (Leuranguer et al., 2001). Therefore, identifying a more selective T-type Ca^{2+} channel antagonist will be useful for the study of cardiac voltage-gated calcium channels and may promote the development of a new class of therapeutically beneficial compounds.

In a previous study, we demonstrated that hydrolysis of the ester side chain of mibefradil resulted in a compound (dm-mibefradil or Ro 40-5966) that exhibited an L-type Ca^{2+} channel-specific inhibitory effect (Wu et al., 2000). We thus proposed that modifications in this ester side chain, which decreased hydrolysis, might result in compounds with lower potency in blocking L-type Ca^{2+} channels and selective action on T-type channels. To test this hypothesis, we examined the effects of several novel mibefradil derivates on T-type and HVA Ca^{2+} currents, in whole cell voltage-clamp recordings. We used HEK 293 cells stably transfected with the α_1G subtype of T-type Ca^{2+} channel (HEK/α_1G) and INS-1 cells to test the effects of our new compounds on T-type and HVA Ca^{2+} channels, respectively. INS-1 cells express a variety of HVA Ca^{2+} current including P/Q-, N-, L- and R-types (Horvath et al.1998), with α_1D contributing majority of the currents (Liu et al., 2002; Huang et al., 2004).

Materials and Methods

Cell Culture. INS-1 cells, an insulin-secreting cell line derived from rat pancreatic beta cells (Asfari et al., 1992) were cultured in RPMI 1640 medium containing 10% fetal bovine serum, 100 U/ml penicillin, 100 μg/ml streptomycin and 50 μ□ ˜mercaptoethanol in an atmosphere of 5% CO_2 in air at 37°C for 2-5 days before recording.

Creation of HEK293 cell lines stably expressing recombinant T-type Ca^{2+} channels. An α_1G cDNA originally cloned from rat pancreatic β-cells (Zhuang et al., 2000), in vector pcDNA3.1 hygro(-) (Invitrogen, Burlington, Ontario), was transfected into HEK cells using the FuGene kit (Roche Diagnostics, Laval, QC). Cell lines stably expressing $Ca_v3.1$ were obtained after transfection using standard cell cloning techniques (Freshney 1983). HEK 293 cells stably-transfected with α_1G cDNA (HEK 293/α_1G) were incubated in DMEM, supplemented with 10% fetal bovine serum, 100 U/ml penicillin, 100 μg/ml streptomycin, and 0.5 mg/ml hygromycin-B in an atmosphere of 5% CO2 in air at 37oC for 2-5 days before recording.

Electrophysiological recording. Whole-cell recordings were carried out by the standard "giga-seal" patch-clamp technique. The whole-cell recording pipettes were made of hemocapillaries (Warner Instrument Corp., Hamden, CT), pulled by a two-stage puller (PC-10; Narishige Interational, NY) and heat polished with a microforge (MF-200; World Precision Instruments, Sarasota, FL) before use. Pipette resistance was in the range of 2 to 5 MΩ in our internal solution. The recordings were performed at room temperature (22-25°C). Electrical currents were recorded using an EPC-9 patch-clamp amplifier (HEKA, Lambrecht/Pfalz, Germany) and filtered at 2.9 kHz. Data were acquired with Pulse/PulseFit software (HEKA).

JPET Fast Forward. Published on January 12, 2004 as DOI: 10.1124/jpet.103.060814
This article has not been copyedited and formatted. The final version may differ from this version.

Voltage-dependent currents were corrected for linear leak and residual capacitance by using an on-line P/n subtraction paradigm. In the whole-cell configuration, T-type Ca^{2+} currents were recorded at -30 mV when the holding potential was –70 mV. The HVA Ca^{2+} current was measured at 20 mV with a holding potential of -40 mV.

Solutions. The extracellular solution used in the whole-cell Ca^{2+} current recording contained 10 mM $CaCl_2$, 110 mM tetraethylammonium-Cl, 10 mM CsCl, 10 mM HEPES, 40 mM sucrose, 0.5 mM 3,4-diaminopyridine, pH 7.3. The intracellular solution contained 130 mM *N*-methyl-D-glucamine, 20 mM EGTA (free acid), 5 mM 1,2-bis(2-aminophenoxy)ethane-*N, N, N' N'*-tetraacetate (BAPTA), 10 mM HEPES, 6 mM $MgCl_2$, and 4 mM $Ca(OH)_2$, with pH adjusted to 7.4 with methanesulfonate. Mg-ATP (2 mM) was included in the pipette solution to minimize "run-down" of L-type Ca^{2+} currents. For perforated-patch experiments, nystatin (200 μg/ml) was used. The pipette was filled with nystatin-containing intracellular solution and gentle suction was used to achieve gigaohm resistance. The access resistance gradually decreased within 5 min after the gigaohm-seal formation, and then currents were recorded after stabilization. The extracellular solution contained 26 mM sucrose, 130 mM tetraethylammonium-Cl, 10 mM HEPES, 5 mM KCl, 2 mM $CaCl_2$, 2 mM $MgCl_2$, pH 7.3. The pipette solution contained 65 mM CsOH, 65 mM Cs-methanesulfonate, 20 mM sucrose, 10 mM HEPES, 10 mM $MgCl_2$, and 1 mM $Ca(OH)_2$, with pH 7.4.

Mass spectrometric analysis. Mass Spectrometric analysis was performed on Perseptive Biosystem Voyager-DE Maldi-TOF instrument (Perseptive Biosystem, Foster, CA). Cultured INS-1 cells were treated with 20 μM NNC 55-0396 for various lengths of time under each

JPET Fast Forward. Published on January 12, 2004 as DOI: 10.1124/jpet.103.060814
This article has not been copyedited and formatted. The final version may differ from this version.

experimental condition. After incubated, cells were washed with PBS three times, scraped into eppendorf tubes with 1 ml of PBS, and centrifuged at 1000 g for 5 min. The cell pellets were collected and re-dissolved by sonication (10 sec) in 0.5 ml of PBS for mass spectrometric analysis. The sample was taken up in alpha-cyano-4-hydroxcinnamic acid (Aldrich, Milwaukee, MI), which was used as the matrix. Ten μl of each sample was mixed with 70 μl of the matrix. One μl of the mixture was spotted on a plate for analysis on the Maldi-TOF instrument. Several positive ion spectra were recorded in the mass range m/z 820 to 99 at a mass resolution of 1000 and a scan speed of 2 s/decade. For NNC 55-0396, m/z 492 was the dominant ion (M+H). For calibration, a standard solution of 50 μM NNC 55-0396 was subjected to mass spectrometric analysis. The relative amount of NNC 55-0396 was determined by calibrating the intensities of NNC 55-0396 with the intensity of standard solution.

Statistics and curve fitting. Nonlinear regression analysis was used to fit concentration-response data to a sigmoid relationship Y=100/(1+10^((LogIC_{50}-X)slope), where slope is the Hill slope parameter, IC_{50} is the concentration producing 50% blockage and X is the drug concentration. Voltage dependent activation and steady state inactivation curves were generated by normalizing the currents with the maximal amplitude in each cell and fitting the data with the Boltzmann equation, 1/(1+exp((V-$V_{1/2}$)/k), where k represents the slope and $V_{1/2}$ represents the voltage corresponding to half activation of the channels. Student *t* test was used to compare $V_{1/2}$ and k values determined from fits of the data with this equation. The data fitting and statistical analysis were performed with the Prism version 4 (GraphPad Software. San Diego, CA). In the figures where the data are presented as symbols and error bars, the values are mean ± SEM.

JPET Fast Forward. Published on January 12, 2004 as DOI: 10.1124/jpet.103.060814
This article has not been copyedited and formatted. The final version may differ from this version.

General chemical procedure. Reagents, starting materials and solvents were purchased from common commercial suppliers and were used as received. All dry solvents were dried over molecular sieves (0.3 or 0.4 nm). Evaporation was carried out on a rotary evaporator at bath temperatures < 40°C and under appropriate vacuum. Flash chromatography was carried out on a Biotage flash 40 using Biotage flash columns (KP-SIL, 60Å particle size 32-63 µM). Melting points were determined with a Büchi B545 apparatus and are uncorrected. Proton NMR spectra were recorded at ambient temperature using a Brucker Avance DPX 200 (200 MHz) and Brucker Avance DPX 300 (300 MHz) with tetramethylsilane as an internal standard for proton spectra,. Chemical shifts are given in ppm (δ) and splitting patterns are designated as follows: s, singlet; d, doublet; dd, double doublet; t, triplet; dt, double triplet; q, quartet; quint, quintet; m, multiplet, and br = broad. The 70 eV E.I. solid mass spectra were recorded on a Finnigan MAT-TSQ 70 mass spectrometer. Reactions were followed by thin layer chromatography performed on silica gel 60 F254 (Merck) or ALUGRAM®SIL G/UV_{254} (MACHEREY-NAGEL) TLC aluminum sheets.

Synthesis of NNC 55-0396 ((1S, 2S)-2-(2-{N-[(3-benzoimidazol-2-yl)propyl]-N-methylamino}ethyl)-6-fluoro-1,2,3,4-tetrahydro-1-isopropyl-2-naphtyl cyclopropanecarboxylate dihydrochloride). Methoxyacetic acid 2(S)-[2-[N-[3-(2-benzimidazolyl)propyl]-N-methylamino]ethyl]-6-fluoro-1(S)-isopropyl-1,2,3,4-tetrahydro-2-naphthyl ester dihydrochloride (mibefradil, 0.570g) in ethanol (96%, 5 ml) and aqueous sodium hydroxide (1 N, 5 ml) was refluxed for 2 h. The cold reaction mixture was concentrated *in vacou*. The residue was partitioned between water and dichloromethane. The aqueous layer was extracted with dichloromethane. The combined organic layers were dried with sodium sulfate and concentrated

JPET Fast Forward. Published on January 12, 2004 as DOI: 10.1124/jpet.103.060814
This article has not been copyedited and formatted. The final version may differ from this version.

to give 2-(2-[[3-(1-benzoimidazol-2-yl)-propyl]methylamino]ethyl)-6-fluoro-1-isopropyl-1,2,3,4-tetrahydro-2-naphthalinol as a clear syrup 0.43g (100%). ^{1}H-NMR ($CDCl_3$): δ 7.57 (broad, 2H); 7.23 (m, 2H); 6.97 (m, 1H); 6.58 (m, 2H); 3.07-2.83 (m, 3H); 2.75 (m, 1H); 2.6 (m, 4H); 2.5-2.2 (s + m, 3H +3H); 2.06 (quint, 2H); 1.81 (broad dd, 1H); 1.50 (m, 2H); 1.20 (d, 3H); 0.53 ppm (d, 3H).

2-(2-{[3-(1-Benzoimidazol-2-yl)-propyl]methylamino}ethyl)-6-fluoro-1-isopropyl-1,2,3,4-tetrahydro-2-naphthalinol (0.110g) was dissolved in dichloromethane (1 ml). Diisopropylethylamine (0.045 ml) and cyclopropanecarbonyl chloride (0.071 ml) was added. After stirring for 19 h the reaction mixture aqueous saturated sodium hydrogencarbonate was added. The aqueous layer was extracted twice with dichloromethane. The combined organic layers were dried with sodium sulfate and concentrated *in vacou*. The residue was purified by flash chromatography using dichloromethane/methanol 6:1 as eluent to give the free base as a syrup. This product was dissolved in ethanol and aqueous hydrochloride (1 N, 0.38 ml) was added. After stirring for 30 min the mixture was concentrated. The residue was crystallized from ethyl acetate to give the title compound as a white powder (50 mg, 34%). Mp: 134-141°C. EI SP/MS: 491 (M+). ^{1}H-NMR (DMSO, d6): δ 7.77 (m, 2H); 7.52 (m, 2H); 7.07 (m, 1H); 6.96 (broad d, 2H); 3.3 (m, 2H); 3.2 (m, 4H); 3.0 (m, 2H); 2.9 (m, 1H); 2.67 (s, 3H); 2.45 (m, 1H); 2.38 (m, 2H); 2.15-1.45 (m, 4H);1.57 (m, 1H); 1.04 (d, 3H); 0.90 (m, 4H); 0.48 ppm (d, 3H).

Synthesis of NNC 55-0395 (1S,2S)-2-(2-(N-[(3-benzoimidazol-2-yl)propyl]-N-methylamino)ethyl)-6-fluoro-1,2,3,4-tetrahydro-1-isopropyl-2-naphtyl valeroate dihydrochloride). The compound was prepared by an analogous procedure: Mp 118-121°C. EI

SP/MS: 507 (M+).^{1}H-NMR (DMSO-d_6): δ 7.75 (m, 2H); 7.49 (m, 2H); 7.08 (m, 1H); 6.96 (broad d, 2H); 3.15 (m, 4H); 2.95 (m, 3H); 2.7 (s, 3H); 2.48 (dt, 2H); 2.23 (m, 2H); 2.0 (m, 4H); 1.50 (p, 2H); 1.35 (quint, 2H); 1.02 (d, 3H); 0.90 (t, 3H); 0.35 ppm (d, 3H).

Synthesis of NNC 55-0397 ((1S,2S)-2-(2-(N-[(3-benzoimidazol-2-yl)propyl]-N-methylamino)ethyl)-6-fluoro-1,2,3,4-tetrahydro-1-isopropyl-2-naphtyl isobutyrate dihydrochloride). The compound was prepared by an analogous procedure: Mp 114-117°C.EI SP/MS: 493 (M+). ^{1}H-NMR (DMSO-d_6): δ 7.77 (m, 2H); 7.52 (m, 2H); 7.07 (m, 1H); 6.96 (broad d, 2H); 3.43 (m, 1H); 3.3- 3.05 (m, 5H); 2.97 (m, 2H); 2.88 (m, 1H); 2.70 (s, 3H); 2.61 (m, 1H); 2.45 (m, 1H); 2.3 (m, 2H);2.15-1.85 (m, 4H); 1.15 (d, 6H); 1.00 (d, 3H); 0.45 ppm (d, 3H).

Results

Synthesis of NNC 55-0396 and other mibefradil analogues. We synthesized three analogues of mibefradil by replacing the ester chain (methoxyacetyl) group: NNC 55-0395, NNC 55-0396, and NNC 55-0397 (Fig. 1). All compounds were synthesized from mibefradil in two steps. Alkaline hydrolysis of mibefradil and subsequent treatment with valeroylchloride, cyclopropanecarbonyl chloride and isobutyrylchloride gave the desired compounds NNC 55-0395, NNC 55-0396 and NNC 55-0397, respectively, upon work-up.

Pharmacological screening effect of NNC 55-0395, NNC 55-0396, and NNC 55-0397 on T-type and HVA Ca^{2+} currents. We used perforated whole-cell patch-clamp to examine the effects of NNC 55-0395, NNC 55-0396 and NNC 55-0397 on HVA Ca^{2+} current in INS-1 cells. In these experiments, the resting membrane potential was held at -40 mV to eliminate T-type Ca^{2+} current. The inhibitory potency of the mibefradil analogues on HVA Ca^{2+} current was examined at dosages of 0.1 μM, 1 μM, 10 μM, 100 μM approximately 10 minutes after the drug perfusion. The results showed that both NNC 55-0395 and NNC 55-0397 had inhibitory effect on HVA Ca^{2+} currents at 100 μM (Figure 2A, 2C), whereas no inhibition on the HVA Ca^{2+} current was detected with NNC 55-0396 at the same concentration (Figure 2B).

Next we determined the effects of NNC 55-0395, NNC 55-0396 and NNC 55-0397 on T-type Ca^{2+} current. These experiments were conducted by measuring the effects of the compounds on whole-cell current in HEK 293/α_1G cells. The dose-dependent inhibition of compounds NNC 55-0395, NNC 55-0396 and NNC 55-0397 on T-type Ca^{2+} current was examined at dosages ranging from 1 to 100 μM. NNC 55-0396 and NNC 55-0397 blocked more than 50% of the T-

JPET Fast Forward. Published on January 12, 2004 as DOI: 10.1124/jpet.103.060814
This article has not been copyedited and formatted. The final version may differ from this version.

type Ca^{2+} current at 8 μM (Figure 2E, 2F), whereas NNC 55-0395 inhibited less than 50% of the T-type Ca^{2+} current at 64 μM (Figure 2D).

Both NNC 55-0395 and NNC 55-0397 blocked HVA Ca^{2+} channel currents in our screening experiments, and thus were eliminated from further characterization. Compound NNC 55-0396, which blocked T-type Ca^{2+} current but not HVA Ca^{2+} currents, was selected for subsequent analysis.

Characterization of the inhibitory effects of NNC 55-0396 on T-type Ca^{2+} current. To further characterize NNC 55-0396, we used whole-cell patch-clamp and a bath perfusion system to examine its dose-dependent effects on T-type and HVA Ca^{2+} currents. At 8 μM, NNC 55-0396 reduced more than 50% of the peak of T-type Ca^{2+} current compared with control in HEK 293/α_1G cells (Figure 3A); however, NNC 55-0396 at 100 μM did not block the HVA Ca^{2+} current in INS-1 cells (Figure 3B), whereas this HVA Ca^{2+} current could be inhibited by 10 μM nifedipine, a selective L-type Ca^{2+} channel blocker (Figure 3C). Pooled data of the effects of NNC 55-0396 on T-type and HVA Ca^{2+} currents are shown in Figure 3D. After bathing HEK 293/α_1G cells with NNC 55-0396 at 8 μM or bathing INS-1 cells with NNC 55-0396 at 100 μM for over 8 minutes, T-type Ca^{2+} currents were inhibited in 60% whereas no decrease in the HVA Ca^{2+} current was observed.

The inhibitory potency of NNC 55-0396 on T-type Ca^{2+} currents in HEK 293/α_1G was also compared with that of mibefradil as shown in Figure 3E. By fitting the data with a sigmoid dose-response relationship equation, NNC 55-0396 and mibefradil blocked T-type Ca^{2+} current

JPET Fast Forward. Published on January 12, 2004 as DOI: 10.1124/jpet.103.060814
This article has not been copyedited and formatted. The final version may differ from this version.

with IC_{50}s of 6.8 and 10.08, respectively. This result suggests that NNC 55-0396 retains potency similar to mibefradil as an inhibitor of T-type Ca^{2+} current.

Long-term exposure of HEK/α_1G cells to NNC 55-0396 showed a decrease in current density of T-type Ca^{2+} channels. Using whole cell patch clamp, we measured T-type Ca^{2+} current density in the HEK/α_1G cells that had bathed in the extracellular solutions containing 0, 10, 100 and 1000 nM NNC 55-0396 for 30-60 minutes (Figure 3F). All peak-current amplitudes and slow capacitances were obtained during the first minute after breaking-in, thus the effect of frequency-dependent inhibitory effect was minimal. Our data showed a slow, yet more potent inhibitory effect of NNC 55-0396 on the T-type Ca^{2+} currents.

Figure 4A illustrates that there was no significant difference in the conductance-voltage relationship (G/V) curves of T-type Ca^{2+} currents between the control cells and cells incubated with 8 μM NNC 55-0396. The conductance (G) was calculated from the current (I) divided by the driving force ($V_{drive} = V_{membrane} - V_{reversal}$), where the $V_{reversal}$ was hypothetically assigned as 70 mV. Curves were generated by fitting the data with the Boltzmann equation. The $V_{1/2}$ and k values are -32.61 ± 1.0 and 4.16 ± 0.9 for the controls (n = 3) and –32.12 ± 0.8 and 4.33 ± 0.73 for cells incubated with NNC 55-0396 (n = 3), respectively. The steady state inactivation curves of T-type Ca^{2+} current were also generated with the Boltzmann equation (Figure 4B). The$V_{1/2}$ values are –59.21 ± 0.38 and –62.84 ± 0.94 for the controls (n = 4) and cells incubated with NNC 55-0396 (n = 6), respectively. The slope k values are 4.92 ± 0.33 with a 95% confidence interval between 4.16 to 5.69 for controls and 7.95 ± 0.72 with a 95% confidence interval between 6.31 to 9.58 for cells incubated with NNC 55-0396, respectively. Therefore, the steady state

inactivation curve of T-type Ca^{2+} current is flattened when NNC 55-0396 is present.

State-dependent block of T-type Ca^{2+} current by NNC 55-0396. The inhibitory mechanism of NNC 55-0396 on T-type Ca^{2+} current was further investigated by testing the effect of changing the holding potential and stimulation frequency. As shown in Figure 5A, in the absence of NNC 55-0396, changing holding potential from –120 mV to –80 mV did not alter the peak amplitude of T-type Ca^{2+} current in an HEK 293/α_1G cell, elicited by depolarizations to –10 mV every 10 seconds. In contrast, after addition of 8 μM NNC 55-0396, switching the membrane potential from –80 mV to –120 mV caused an increase in the current amplitude, suggesting a partial relief of block at the more hyperpolarized holding potential. Similarly, increasing pulse rate from 0.05 Hz to 0.5 Hz had little effect on current amplitude without NNC 55-0396, whereas the rate of inhibition of T-type Ca^{2+} current was accelerated by increasing the frequency of stimulation in the presence of drug (Figure 5B). Similar results of both voltage-dependent and frequency dependent blockade were observed in four experiments.

Mass spectrometric analysis of NNC 55-0396 treated INS-1 cells. Previously we found that mibefradil blocked both T-type and HVA Ca^{2+} current in INS-1 cells (Wu et al., 2000). After entering the cells, mibefradil is broken down into metabolites. One of them is des-methoxyacetyl mibefradil, which exerts an inhibitory effect on HVA Ca^{2+} channels by acting on the channels from inside the cell. To investigate why NNC 55-0396 and mibefradil have different effects on HVA Ca^{2+} channels, we used mass spectrometric analysis to examine whether des-methoxyacetyl mibefradil was produced intracellularly when the cells were treated with NNC 55-0396. Figure 6A shows a section of mass spectrum of molecules in INS-1 cells that had

JPET Fast Forward. Published on January 12, 2004 as DOI: 10.1124/jpet.103.060814
This article has not been copyedited and formatted. The final version may differ from this version.

been incubated with NNC 55-0396 for 20 minutes. Notably, no des-methoxyacetyl mibefradil (which peaks at 424 m/z) was detected in this preparation. This finding suggests that unlike mibefradil, the compound NNC 55-0396 is not hydrolyzed into des-methoxyacetyl mibefradil. Thus, NNC 55-0396 does not inhibit HVA Ca^{2+} channels as mibefradil does. The amount of NNC 55-0396 (which peaks at 492 m/z), however, increased in the cells with periods were longer than 10 minutes as shown in Figure 6B.

Accessibility of NNC 55-0396 on the T-type Ca^{2+} channel. The slow onset of NNC 55-0396 inhibition on T-type Ca^{2+} current and the increasing NNC 55-0396 accumulation in the cells with time suggest that this compound dissolves in or pass through the plasma membrane to exert its effect. To test this hypothesis, we examined the reversibility of NNC 55-0396 blockade of T-type Ca^{2+} current. Whole cell currents were evoked in HEK 293/α_1G cells by test pulses to –10 mV from a holding potential of –70 mV. After establishing a steady current, small volumes of 8 μM NNC 55-0396 were delivered in close proximity to the recording cell with a quartz capillary positioned by a micromanipulator. The drug was washed out after more than 50% inhibition of T-type Ca^{2+} current was achieved. As shown in Figure 7A, the blockade of the T-type Ca^{2+} current by NNC 55-0396 was poorly reversible during a 10 minute washout period in these experiments. Since the NNC 55-0396 blocks T-type Ca^{2+} current in a relative slow rate and is poorly reversible by washing out, the drug binding site of the channel may be within transmembrane domains or intracellular domains of the channel.

If the site of action of NNC 55-0396 is on the intracellular side of the membrane, we would expect that intracellular perfusion of the drug would effectively block T-type Ca^{2+} current.

JPET Fast Forward. Published on January 12, 2004 as DOI: 10.1124/jpet.103.060814
This article has not been copyedited and formatted. The final version may differ from this version.

To test this possibility, whole cell currents were recorded in HEK 293/α_1G cells with 8 μM NNC 55-0396 added to the pipette solution. As shown in Figure 7B, there was no significant difference between the current in HEK 293/α_1G cells with (n = 10) and without (n = 6) NNC 55-0396 included in the pipette solution. For example, at the 10 minute time point, the p value is 0.12 with two tailed-unpaired *t* test analysis. These data are inconsistent with the idea that the site of action of NNC 55-0396 is on the cytoplasmic face of the T-type Ca^{2+} channel. Thus, NNC 55-0396 appears to exhibit a relatively slow and wash-resistant binding to a site, perhaps within the transmembrane domains of the channel.

JPET Fast Forward. Published on January 12, 2004 as DOI: 10.1124/jpet.103.060814
This article has not been copyedited and formatted. The final version may differ from this version.

Discussion

Mibefradil blocks both T-type Ca^{2+} channels and HVA Ca^{2+} channels. Although mibefradil appears to act directly on T-type channels, we previously reported that its effect on HVA channels is not direct, but instead involves cell permeation and hydrolysis to an active metabolite that acts from the cytoplasmic side of the membrane (Wu et al, 2000). In the present study we developed a new compound, NNC 55-0396, which has an inhibitory effect on T-type Ca^{2+} current in HEK/α_1G cells, but is not hydrolyzed to an active metabolite and does not block HVA Ca^{2+} currents in INS-1 cells. Thus, NNC 55-0396 is a selective inhibitor for T-type Ca^{2+} channels. Our data also suggest that the effect of NNC 55-0396 on T-type channels is state-dependent: block is partially relieved by membrane hyperpolarization and enhanced by high frequency channel activation.

Our previous findings (Wu et al., 2000) suggest that the methoxyacetyl group of mibefradil is a critical determinant for binding to HVA channels, since its hydrolysis is the critical step in binding of the compound to HVA channels. In contrast, this moiety may play only a modest role in interacting with the receptor domain of T-type Ca^{2+} channels, since all three alternations, NNC 55-0395, NNC 55-0396 and NNC 55-0397, retain the capability of blocking T-type Ca^{2+} current, although with varying potency. Our study indicates that modification in the methoxyacetyl group of mibefradil can improve its selectivity for T-type Ca^{2+} channels over the HVA Ca^{2+} channels without sacrificing the potency of T-type Ca^{2+} channel antagonism.

The primary objective of this study is to examine the structure-selectivity relationship of a small group of mibefradil derivatives. Therefore, we chose HEK/α_1G as a clean model system.

JPET Fast Forward. Published on January 12, 2004 as DOI: 10.1124/jpet.103.060814
This article has not been copyedited and formatted. The final version may differ from this version.

We do not know how effectively NNC 55-0396 will block other T-type Ca^{2+} channels, nor do we know its potency on α_1G when other auxiliary subunits are present. However, we speculate that NNC 55-0396 will block α_1H and α_1I as well, for it has been shown that the IC_{50}s of mibefradil blocking α_1G, α_1H, and α_1I are similar (Martin et al., 2000). In summary our findings represent an important step toward development of a specific T-type Ca^{2+} inhibitor, and thus have potentially important scientific and therapeutic implications.

Acknowledgements

We thank Dr. B. Z. Peterson for his constructive criticism on this work. The mass spectrometric analyses were carried out in the Louisiana State University Health Sciences Center New Orleans Core Laboratories.

References

Armstrong CM and Matteson DR (1985) Two distinct populations of calcium channels in a clonal line of pituitary cells. *Science* 227:65-67.

Asfari M, Janjic D, Meda P, Li G, Halban PA and Wollheim CB (1992) Establishment of 2-mercaptothanol-dependent differentiated insulin-secreting cell lines. *Endocrinol* **130:**167-178.

Bezprozvanny I and Tsien RW (1995) Voltage-dependent blockade of diverse types of voltage-gated Ca^{2+} channes expressed in Xenopus Oocytes by the Ca^{2+} channel antagonist mibefradil (Ro 40-5967). *Mol Pharmacol* 48:540-549.

Bian K and Hermsmeyer K. (1993) Ca^{2+} channel actions of the non-dihydropyridine Ca^{2+} channel antagonist Ro 40-5967 in vascular muscle cells cultured from dog coronary and saphenous arteries. *Naunyn Schmiedebergs Arch Pharmacol* **348:**191-196.

Catterall WA (1998) Structure and function of neuronal Ca^{2+} channels and their role in neurotransmitter release. *Cell Calcium* **24:**307-323.

Cremers B, Flesch M, Sudkamp M and Bohm M (1997) Effects of the novel T-type calcium channel antagonist mibefradil on human myocardial contractility in comparison with nifedipine and verapamil. *J Cardiovasc Pharmacol* **29:**692-696.

Ernst ME and Kelly MW (1998) Mibefradil, a pharmacologically distinct calcium antagonist. *Pharmacotherap* **18:**463-485.

Freshney RI (1983) Culture of Animal Cells. Alan R. Liss, New York. 295 pp.

Horvath A, Szabadkai G, Varnai P, Aranyi T, Wollheim CB, Spat A and Enyedi P (1998) Voltage

dependent calcium channels in adrenal glomerulosa cells and in insulin producing cells". *Cell Calcium* **23:**33-42.

Huang L, Bhattacharjee A, Taylor JT, Keyser BM, Zhang, Marrero ML, M. Li M (2004) $[Ca^{2+}]_i$ regulated $Ca_V1.3$ translocation in insulin secreting cells. *Am J Physiol:Cell Physiol* In press.

Jiménez C, Bourinet E, Leuranguer V, Richard S, Snutch TP and Nargeot J (2000) Determinants of voltage-dependent inactivation affect mibefradil block of calcium channels. *Neuropharmacol* **39:**1-10.

Liu G, Dilmac N, Hilliard N and Hockerman GH (2002) Cav1.3 is preferentially coupled to glucose-stimulated insulin secretion in the pancreatic β-cell line INS-1. J Pharmacol Exp Ther 305:271-278.

Madle A, Linhartova K and Koza J (2001) Effects of the T-type calcium channel blockade with oral mibefradil on the electrophysiologic properties of the human heart. *Med Sci Monit* **7:**74-77.

Martin RL, Lee J-H, Cribbs LL, Perez-Reyes E and Hanck DA (2000) Mibefradil block of cloned T-type calcium channels. *J Pharmacol Exp Ther* **295:**302-308.

McDonough SI and Bean BP (1998) Mibefradil inhibition of T-type calcium channels in cerebellar purkinje neurons. *Mol Pharmacol* **54:**1080-1087.

Mishra SK and Hermsmeyer K (1994) Selective inhibition of T-type Ca^{2+} channels by Ro 40-5967. *Circ Res* **75:**144-148.

Osterrieder W and Holck M (1989) In vitro pharmacological profile of Ro 40-5967, a novel Ca^{2+} channel blocker with potent vasodilator but weak inotropic action. *J Cardiovasc Pharmacol* **13:**754-759.

Perez-Reyes E (1998) Molecular characterization of a novel family of low voltage-activated, T-type, calcium channels. *J Bioenerg Biomembr* **40:**313-318.

Schmitt R, Clozel JP, Iberg N and Buhler FR (1995) Mibefradil prevents neointima formation after vascular injury in rats. Possible role of the blockade of the T-type voltage-opened calcium channel. *Arterioscler Thromb Vasc Biol* **15:**1161-1165,.

Wu S, Zhang M, Vest PA, Bhattacharjee A, Liu L and Li M (2000) A miberfradil metabolite is a potent intracellular blocker of L-type Ca^{2+} currents in pancreatic β-cells. *J Pharmacol Exp Ther* **292:**939-943.

Zhuang, H, Bhattacharjee, A, Hu, F., Zhang, M, Goswami, T, Wang, L, Wu, S., Perggren, P-O, Li, M (2000) Cloning of a T-type Ca^{2+} channel isoform in insulin-secreting cells. *Diabetes* **49:**59-64.

Footnotes:

This study was supported by American Heart Association (0151047B for M.L.) and by Canadian Institutes of Health Research grant MT13485 to D.S.R.

Legends

Figure 1. **Synthesis of NNC 55-0396 and other analogues from mibefradil.** Chemical Structures of NCC 55-0395, NCC 55-0396 and NCC 55-0397. The side chain of mibefradil inside the dashed box is replaced by the new structures indicated by arrows.

Figure 2. **Pharmacological screening effect of NNC 55-0395, NNC 55-0396 and NNC 55-0397 on HVA and T-type Ca^{2+} currents.** A, B and C, dose-dependent effects of the three compounds on HVA currents recorded with perforated whole cell patch clamp in INS-1 cells with a holding potential of -40 mV and a test pulse at 10 mV for 200 ms in every 30-40 seconds. The relative current values were obtained by normalizing the current amplitudes with respect to those recorded under the drug free condition. D, E and F, dose-dependent effects of the three compounds on T-type Ca^{2+} currents recorded with whole cell patch clamp in HEK 293/α_1G cells with a holding potential of -70 mV and a testing potential of -20 mV for 200 ms. n = 3-5 for each set of data.

Figure 3. **The effects of NNC 55-0396 on T-type and HVA Ca^{2+} channels.** A, current traces of T-type Ca^{2+} currents in an HEK 293/α_1G cell before and after application of 8 μM NNC 55-0396. The holding potential was -70 mV and the test potential was -20 mV. B, current traces of HVA Ca^{2+} currents in an INS-1 cell before and after 100 μM NNC 55-0396. The currents were recorded at 10 mV for 200 ms when held at –40 with perforated whole cell patch-clamp. The traces were filtered at 1 kHz. C, a Ca^{2+} current was inhibited by 10 μM nifedipine in an INS-1 cell. The currents were measured at 10 mV before and after nifedipine administration with a holding potential of -70 mV. D, time dependent effects of NNC 55-0396 on HVA and T-

type Ca^{2+} currents. The open circles represent relative currents of HVA Ca^{2+} channels recorded in INS-1 cells before and after 100 μM NNC 55-0396 administration (n = 6), whereas the solid circles represent relative current recorded in HEK 293/α_1G cells before and after 8 μM NNC 55-0396 administration (n = 4). NNC 55-0396 was applied to the bath 3 minutes after the beginning of the recording. E, dose-dependent inhibitory effects of NNC 55-0396 (open circles, n = 6) and mibefradil (Solid circles, n = 4) on T-type Ca^{2+} currents recorded in HEK/α_1G cells. The smooth lines are according to the Hill equation, with IC_{50} values of 6.8 and 10.08 μM for NNC 55-0396 and mibefradil, respectively. The Hill-slopes are –2.39 and –4.26 for NNC 55-0396 and mibefradil, respectively. F, comparison of current densities (pA/pF) among HEK/α_1G cells incubated in various concentrations of NNC 55-0396 for 30-60 minutes. The peak-current amplitudes were measured at -20 mV when held at –70 mV. n = 7-11 for each set of data. Asterisk represents $p < 0.01$ of the data as compared to the control (0 nM NNC 55-0396).

Figure 4. **Effects of NNC 55-0396 on voltage-dependent activation (G/V) and steady state inactivation of T-type Ca^{2+} channel.** A, voltage dependent activation (G/V) curves of T-type Ca^{2+} channel with (solid circles) and without (open circles) presence of 8 μM NNC 55-0396 were fit by Boltzmann equation (n = 3). B, steady state inactivation curves of T-type Ca^{2+} channel with (solid circles) and without (open circles) presence of 8 μM NNC 55-0396 were fit by Boltzmann equation. (n = 6). Steady state inactivation was determined by applying a pre-stimulating pulse of 1.5 second at various voltages immediately before the test pulse at –20 mV. For both A and B, currents were recorded in HEK 293/α_1G cells and the cell membrane was held at –70 mV.

Figure 5. **State-dependent inhibition of T-type Ca^{2+} channels by NNC 55-0396.** A, whole cell Ca^{2+} currents were measured at –10 mV when held at –120 and –80 mV as indicated by the bar above the graph. The pulses were applied every 10 seconds. B, whole cell Ca^{2+} currents were measured at –10 mV when held at –70 mV at stimulation frequencies of 0.05 and 0.5 Hz as indicated by the bar above the graph. NNC and the arrows indicate the time when NNC 55-0396 was perfused into the bath.

Figure 6. **Mass spectrometric analysis of INS-1 cells treated with NNC 55-0396.** A, no ester side chain hydrolytic metabolite (peak is predicted at 424 m/z) was detected in INS-1 cells after 30 minutes incubation with 20 μM of NNC 55-0392, which peaked at 492 m/z. B, time related relative intensity of NNC 55-0396 in INS-1 cells. Mass spectrometry was performed to the cells that had been incubated in 20 μM NNC 55-0396 for various time and then washed three times. The relative intensity is presented as the ratio of the energy power of the laser between the NNC 55-0396 found inside cells and the standard solution containing 50 μM NNC 55-0396. n = 4.

Figure 7. **Washout and intracellular application of NNC 55-0396.** A, inhibitory effect of 8 μM NNC 55-0396 on HEK/α_1G T-type Ca^{2+} currents was not reversed after perfusion with the drug free extracellular solution (n = 3). B, effect of intracellular application of NNC 55-0396 on HEK/α_1G T-type Ca^{2+} currents. The currents were recorded by the whole cell patch-clamp with a pipette solution contained 8 μM NNC 55-0396 (solid circles, n = 10) or a drug free solution (open circles, n = 6). All recording were conducted at holding potential of -70 mV and test pulse of -20 mV.

Figure 1

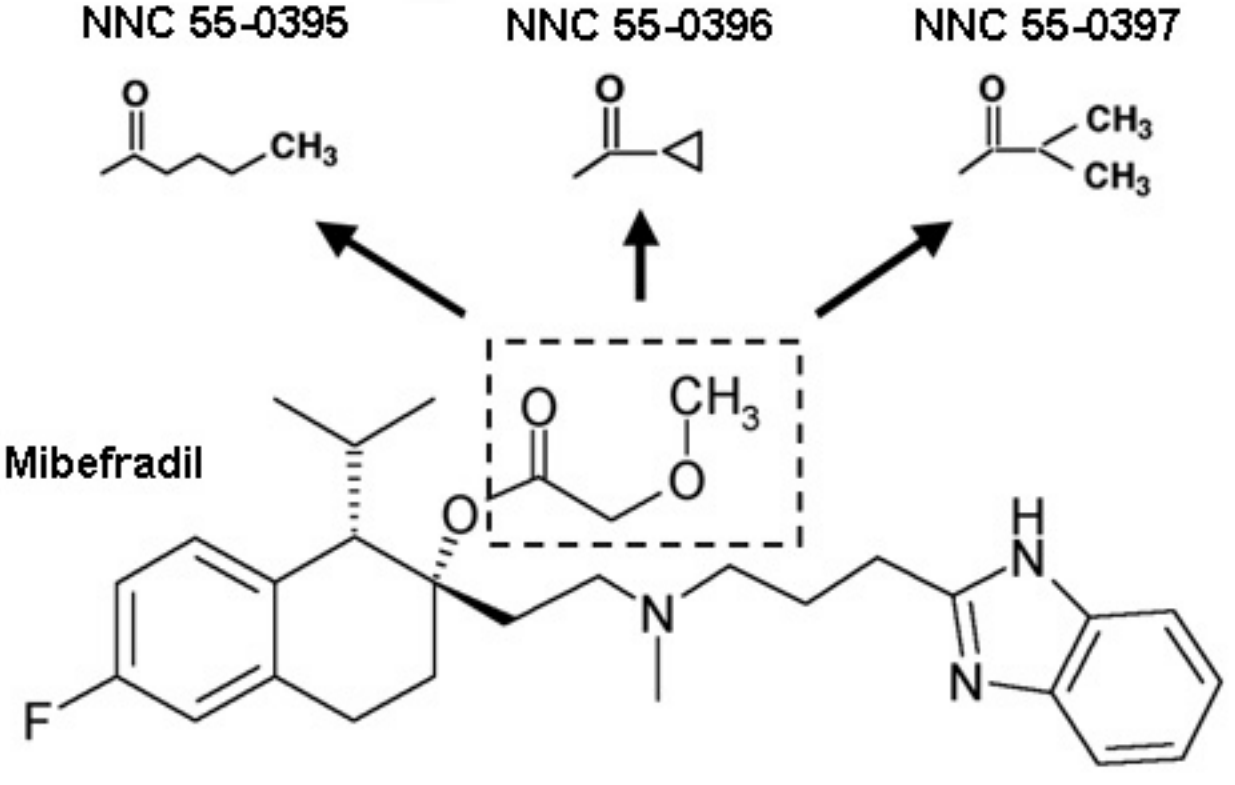

Figure 2

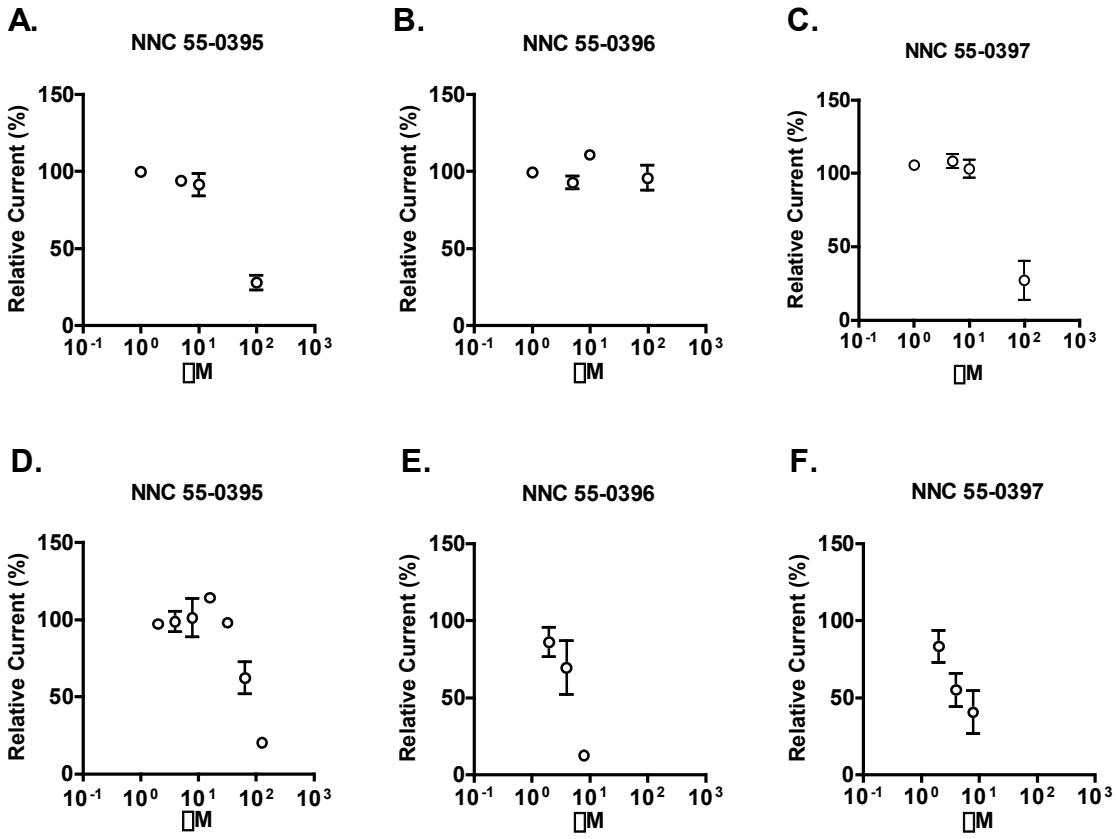

Figure 3

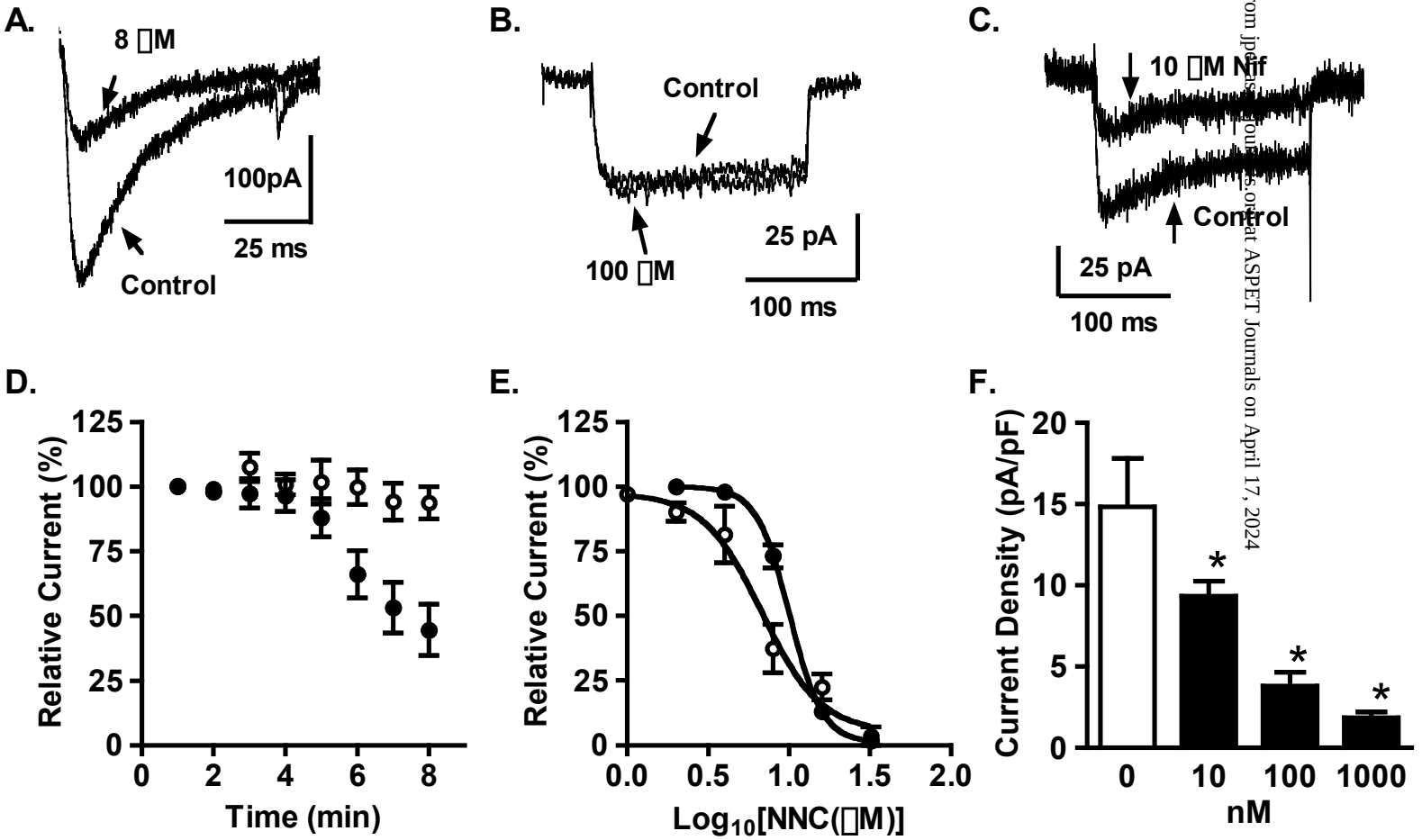

Figure 4

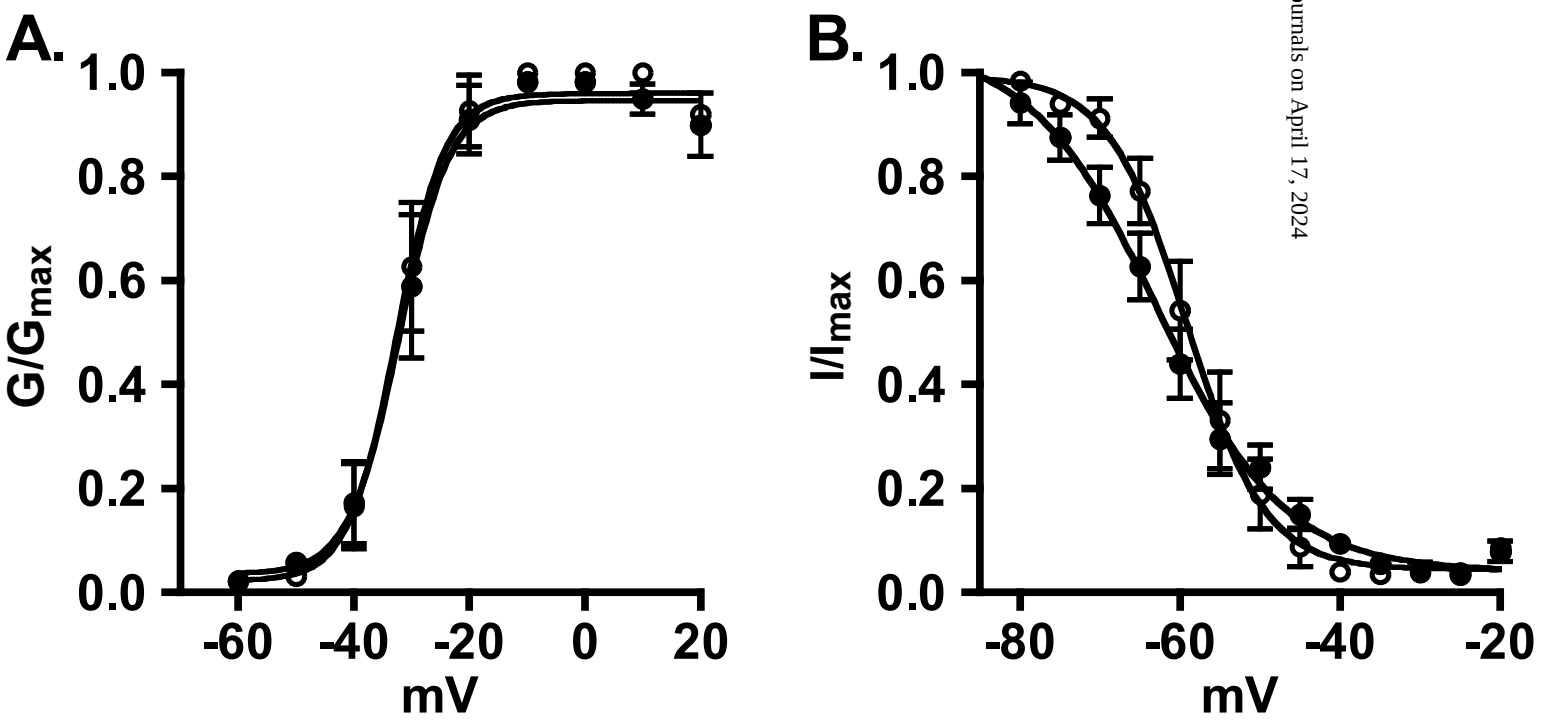

Figure 5

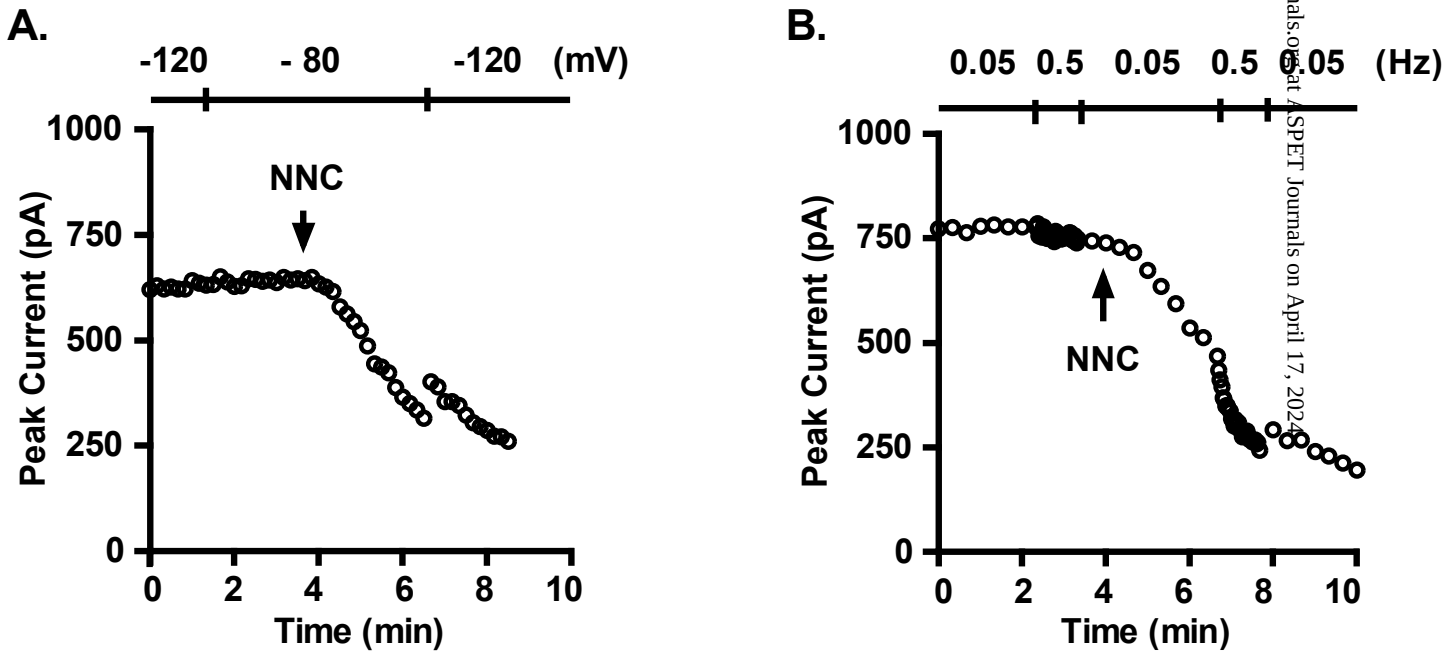

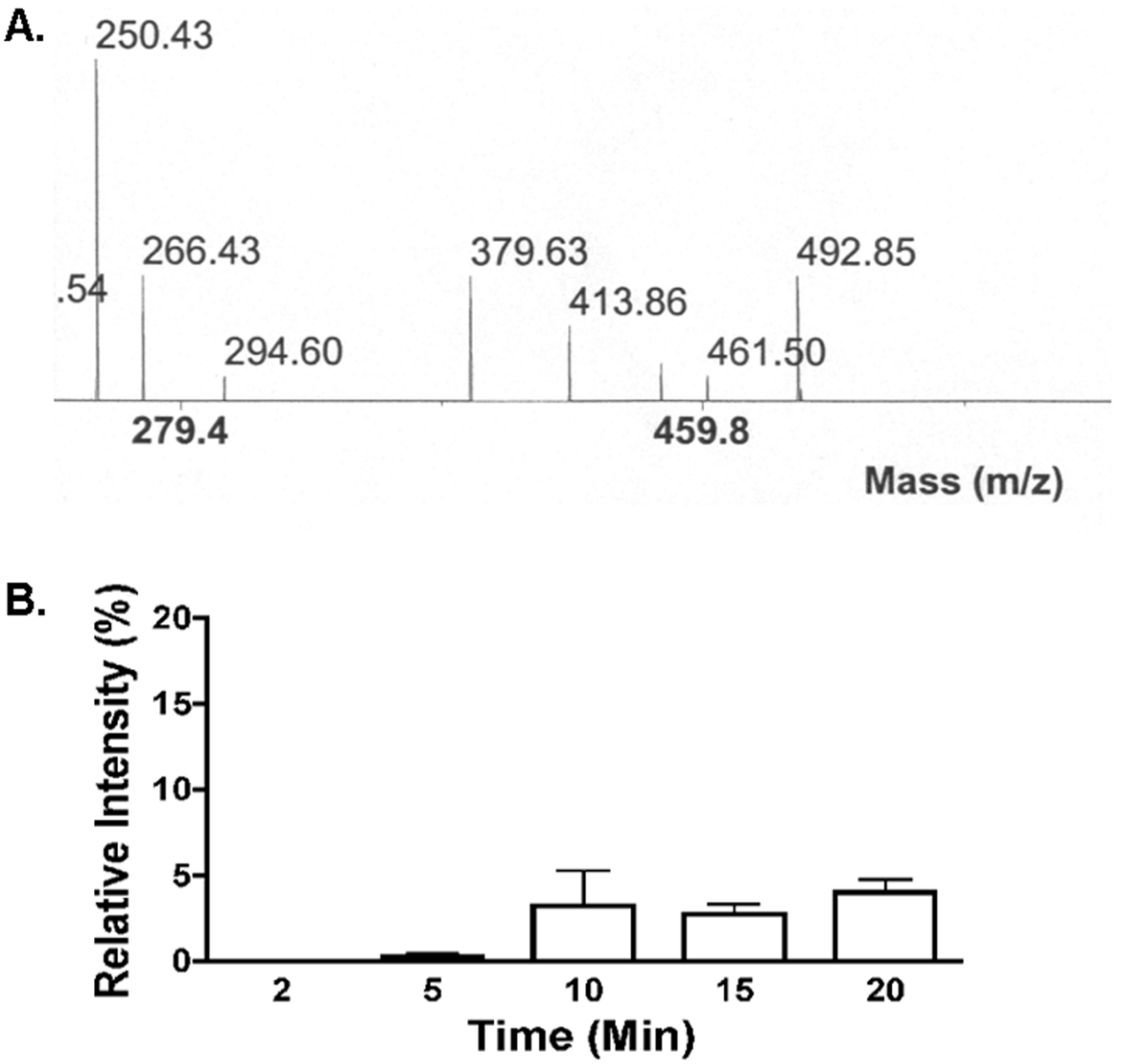
A.
250.43
266.43
379.63
492.85
.54
413.86
294.60
461.50
279.4
459.8
Mass (m/z)
B.
Relative Intensity (%)
20
15
10
5
0
2
5
10
15
20
Time (Min)

Figure 7